

CHAPTER 6

INTERPRETATION OF DOPPLER VELOCITY PATTERNS

6.1 **Introduction.** Although a single Doppler radar observes only the component of the wind in a radial direction from the radar, a wide variety of weather features of great importance can be identified. In this chapter, subjective and objective interpretations of Doppler velocity patterns produced by vertical and horizontal variations of simulated horizontal wind fields are discussed. For the simulated WSR-88D data, Doppler velocity data points were produced at 1.0° increments in the azimuthal direction and 0.13 nm (0.25 km) increments in range. With interest in signature interpretation, an infinitesimally narrow radar beam was used for the simulations so there would not be the increased smearing with range that ordinarily occurs since beam width broadens with increasing range.

Online:

- (From the University of Illinois) Interpreting Doppler Radar Velocities: speed shear wind patterns.

[http://ww2010.atmos.uiuc.edu/\(Gh\)/guides/rs/rad/ptrn/ptrn1.rxml](http://ww2010.atmos.uiuc.edu/(Gh)/guides/rs/rad/ptrn/ptrn1.rxml)

- (From the Weather Decision Training Branch) Go to the updated version of the IC5.4.

<http://wdtb.noaa.gov>

6.2 **Patterns Due to Vertical Variations of the Wind.** Winds that vary with height produce Doppler velocity patterns on a display at a constant elevation angle that can be uniquely interpreted. In these situations, the radar return may be from some combination of refractivity gradients, insects, and/or particulate matter in optically clear air (Appendix B) or from widespread stratiform precipitation. Random noise was added to the simulated Doppler velocity fields to produce more realistic looking Doppler velocity displays.

Consider, for instance, a vertical wind profile where the speed is a constant 45 kts (23 ms^{-1}) and the direction changes uniformly from southerly at the ground to westerly at a height corresponding to the edge of the display (Figures 6-1a and b). With the center of the display representing the radar location, winds that have a component away from the radar have a positive Doppler velocity value (red and orange in Figure 6-1d). Those toward the radar have a negative Doppler velocity value (blue). When the wind direction is normal to the radial direction from the radar, the Doppler velocity component is zero (gray).

Figure 6-1c indicates how to interpret wind direction along the gray zero Doppler velocity band.

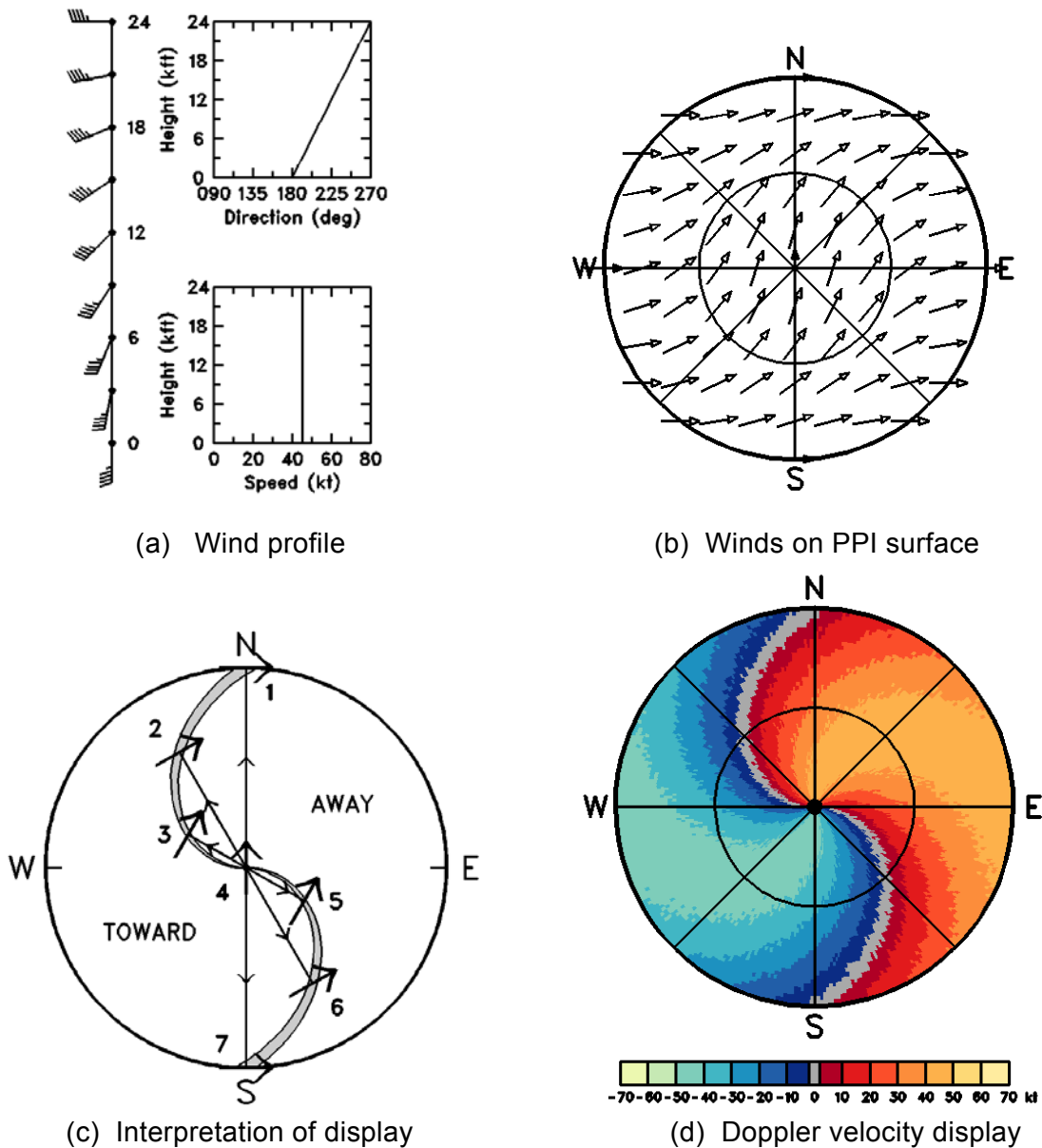


**Figure 6-1
Environmental Wind**

Vertical profile (a) of uniform wind speed (45 kts, 23 ms^{-1}) that veers with height and (b) corresponding horizontal wind vectors on a conical Plan Position Indicator (PPI) surface where height increases from the center of display (ground level) outward. Interpretation of wind direction along the zero Doppler velocity (gray) band in (d) is shown in (c) where bold arrows represent wind vectors. Positive Doppler velocities (red, orange) represent flow away from the radar (at center of display) and negative Doppler velocities (blue) represent flow toward radar.

The presence of the zero band indicates that the wind direction is perpendicular to the radial viewing direction from the radar at that location (that is, wind direction is tangent to the circle at that radius). For example, along the outer edge of the display, the Doppler velocity is zero when the radar points toward the north (point 1) and the south (point 7). This means that the wind is blowing either from west to east or from east to west at the height corresponding to the edge of the display. Since Doppler velocities are negative (component toward the radar) along the western edge of the display and positive (component away from the radar) along the eastern edge, the wind obviously is blowing from west to east at the height of the edge of the display.

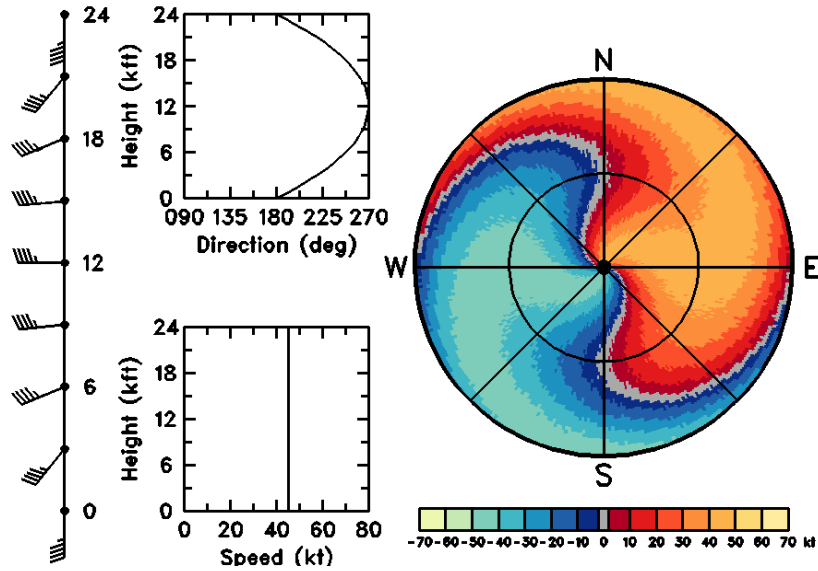
When the radar aims toward point 2 on the zero band, it is pointing toward 330° . The wind direction at that point is $330^\circ \pm 90^\circ$. Since the wind is blowing generally from west to east, the wind at point 2 must be from $330^\circ - 90^\circ = 240^\circ$. Similar arguments at points 3, 5, and 6 result in wind directions of $300^\circ - 90^\circ = 210^\circ$, $120^\circ + 90^\circ = 210^\circ$, and $150^\circ + 90^\circ = 240^\circ$, respectively. At the radar location on the ground (point 4), the zero band is oriented east-west. Since the wind is approaching the radar from the south, wind direction is from 180° .

Wind speed at a given height (slant range) is determined by the extreme Doppler velocity values around a constant slant range circle. In Figure 6-1d, maximum flow away from the radar (light orange) and maximum flow toward the radar (light blue) indicate that wind speed is constant from the ground to the height corresponding to the edge of the display. Thus, the Doppler velocity pattern in Figure 6-1d uniquely represents an environmental wind profile where wind speed is constant and wind direction veers uniformly from southerly at the ground through southwesterly to westerly at the edge of the display.

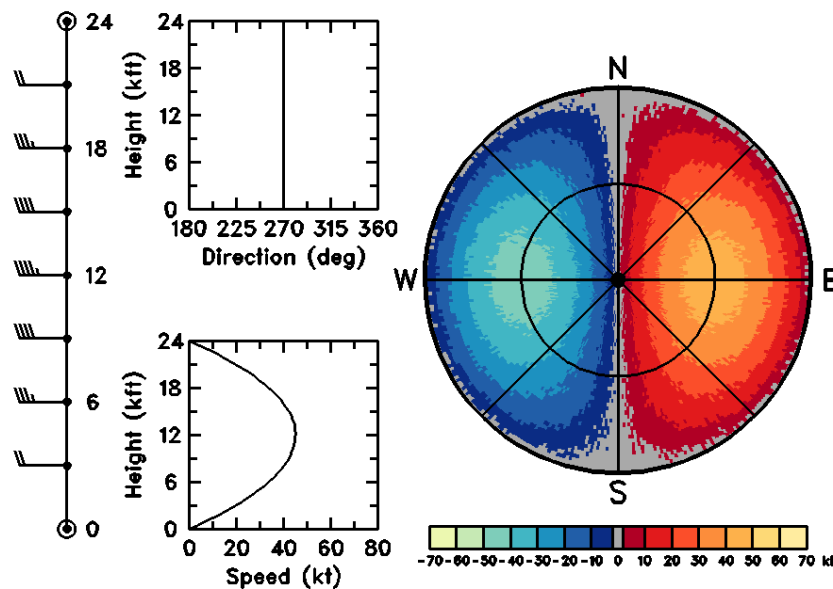
Doppler velocity displays corresponding to a variety of vertical profiles of wind speed and direction are shown in Figure 6-2. When wind speed is constant (non-zero) with height (Figures 6-1d and 6-2a), all of the color velocity bands converge to the radar location at the center of the display. Curvature of the zero Doppler velocity band indicates the change of wind direction with height. Veering winds produce an S-shaped profile (Figure 6-1d) and backing winds produce a backward S-shaped profile (Figure 6-2c). When the wind direction veers then backs with height, an S-shaped profile changes into a backward S-shaped profile with increased range from (height above) the radar (Figure 6-2a).

Doppler velocity patterns associated with the same wind direction at all heights always have a straight zero line (Figure 6-2b). The rest of the pattern reflects the vertical profile of the wind speed. When a wind speed maximum exists within the height interval represented by the display, a pair of quasi-elliptical bull's-eyes appears on the display (Figure 6-2b). The centers of the bull's-eyes are positioned upwind (negative) and downwind (positive) of the radar at the slant range equivalent to the height of the wind maximum. Note that only the zero band passes through the radar location at the center of the display when wind speed is zero at the ground and increases with height.

When wind speed at the ground is less than the maximum value (but still greater than zero), those colors corresponding to wind speeds less than or equal to the surface value converge to the center of the display (Figure 6-2c). Those colors corresponding to greater speeds converge toward the center but never reach it. With wind direction varying with height, the bull's-eye pattern of Figure 6-2b becomes distorted.



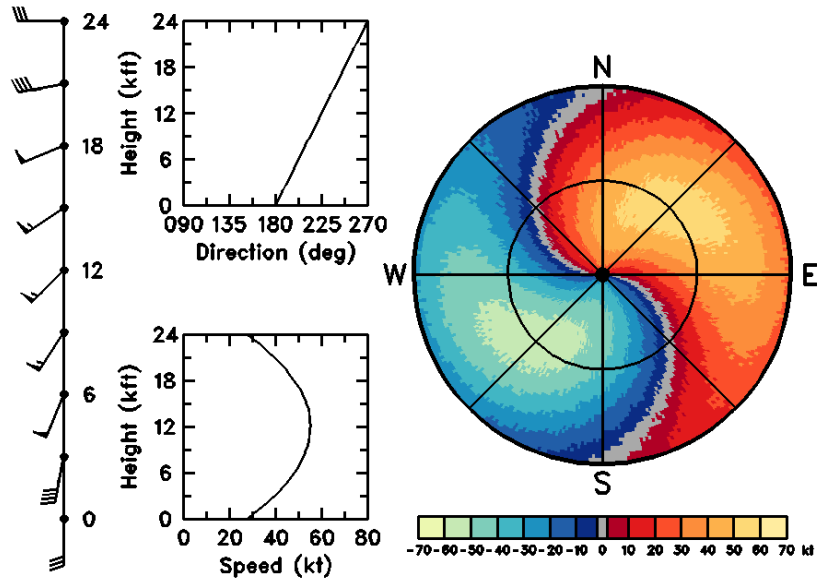
(a) Constant wind speed; wind direction veering, then backing



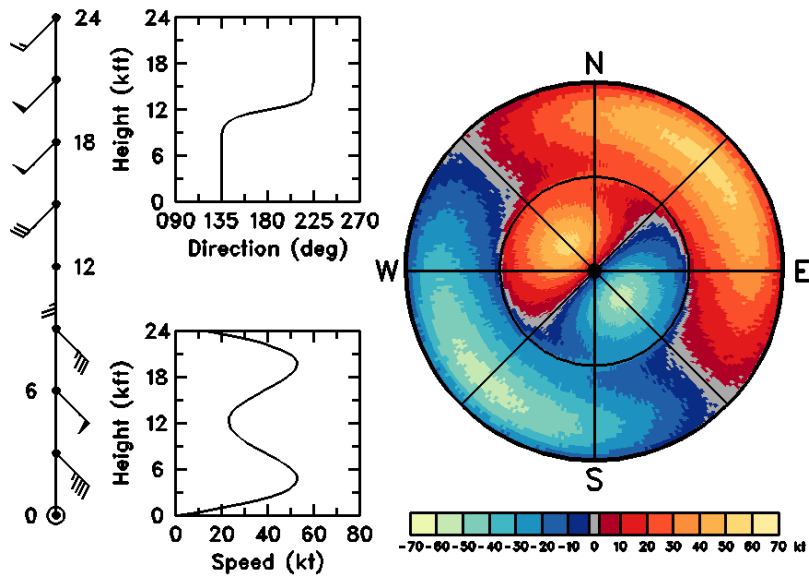
(b) Constant wind direction, middle-altitude speed maximum

Figure 6-2
Variety of Doppler Velocity Displays

Doppler velocity displays corresponding to (a) constant wind speed 45 kts (23 ms^{-1}) with veering at lower altitudes and backing at higher altitudes. (b) Constant wind direction (270°) and middle-altitude speed maximum with calm winds at the ground (display center) and edge of display.



(c) Veering wind direction with middle-altitude speed maximum



(d) Two-layer wind regime, each having constant wind direction and a speed maximum

Figure 6-2
Variety of Doppler Velocity Displays
(concluded)

(c) Veering wind direction and middle-altitude speed maximum 55 kts (28 ms^{-1}) with 30 kts (23 ms^{-1}) winds at the ground and edge of display. (d) Two-layer wind regime with each layer having constant wind direction and a speed maximum 55 kts (28 ms^{-1}) in middle of layer.

Figure 6-2d illustrates an example of Doppler velocity fields through a horizontal surface that separates two different atmospheric flow regimes. There is a wind speed maximum within each wind regime and wind directions differ by 90°. The discontinuity region could represent a frontal surface or it could represent the top of the boundary layer in clear air. Note the variation of the zero Doppler velocity band. It is oriented northeast-southwest through the center of the display indicating a constant wind direction in the lower layer. The inner pair of bull's-eyes indicates that the wind is blowing from the southeast to the northwest at 50–60 kts (26–31 ms⁻¹). The zero velocity band indicates a 90° shift in wind direction through a narrow height interval, with the wind direction becoming constant again above the discontinuity region. The second pair of bull's-eyes indicates that the upper layer winds are from the southwest at 50–60 kts (26–31 ms⁻¹).

There are two important points to remember when attempting to interpret Doppler velocity patterns such as those in Figures 6-2a through d. The first point is that the vertical profile of wind speed is responsible for producing the overall pattern. The surface wind speed is equal to the largest Doppler velocity color band that converges to the radar location at the center of the display. The second point is that the vertical profile of wind direction controls curvature of the color bands. The most informative velocity for interpreting wind direction is the zero Doppler velocity band.

Discontinuities in Doppler velocity patterns frequently are associated with frontal boundaries. With adequate signal return, it is possible to determine characteristics of the flow field both ahead of and behind a front. For example, the pattern in Figure 6-3d clearly indicates that the frontal zone is marked by a rapid change of Doppler velocity over a narrow transition region. As indicated in Figures 6-3a through c, the wind backs and increases in speed with height behind the front and veers and increases with height ahead of the front.

6.3 Quantitative Measurements of Vertical Profiles of the Horizontal Wind. The qualitative interpretation of single Doppler velocity patterns obtained by rotating the radar antenna at one elevation angle has been discussed in Section 6.2. This section investigates a technique for making quantitative measurements from the same data in either optically clear air or widespread precipitation at multiple elevation angles. For this approach, the velocity field is assumed to vary linearly in space. Also, the vertical air motion is assumed to be negligible. The Velocity Azimuth Display (VAD) Algorithm that makes these quantitative measurements on an operational basis is discussed in Part C of this Handbook.

The basic radar scanning geometry is shown in Figure 6-4a. The Doppler velocity, v_d , measurement at height $h = r \sin \alpha$, can be computed from:

$$V_d = V_t \sin \alpha - V_h \cos \alpha \cos \beta,$$

where V_h is the horizontal wind velocity (a positive quantity) at height h and azimuth angle β measured from the upwind direction (maximum flow toward the radar), V_t is the terminal fall velocity (a negative quantity) for precipitation particles in the absence of vertical air motion, and α indicates the elevation angle of the radar antenna.

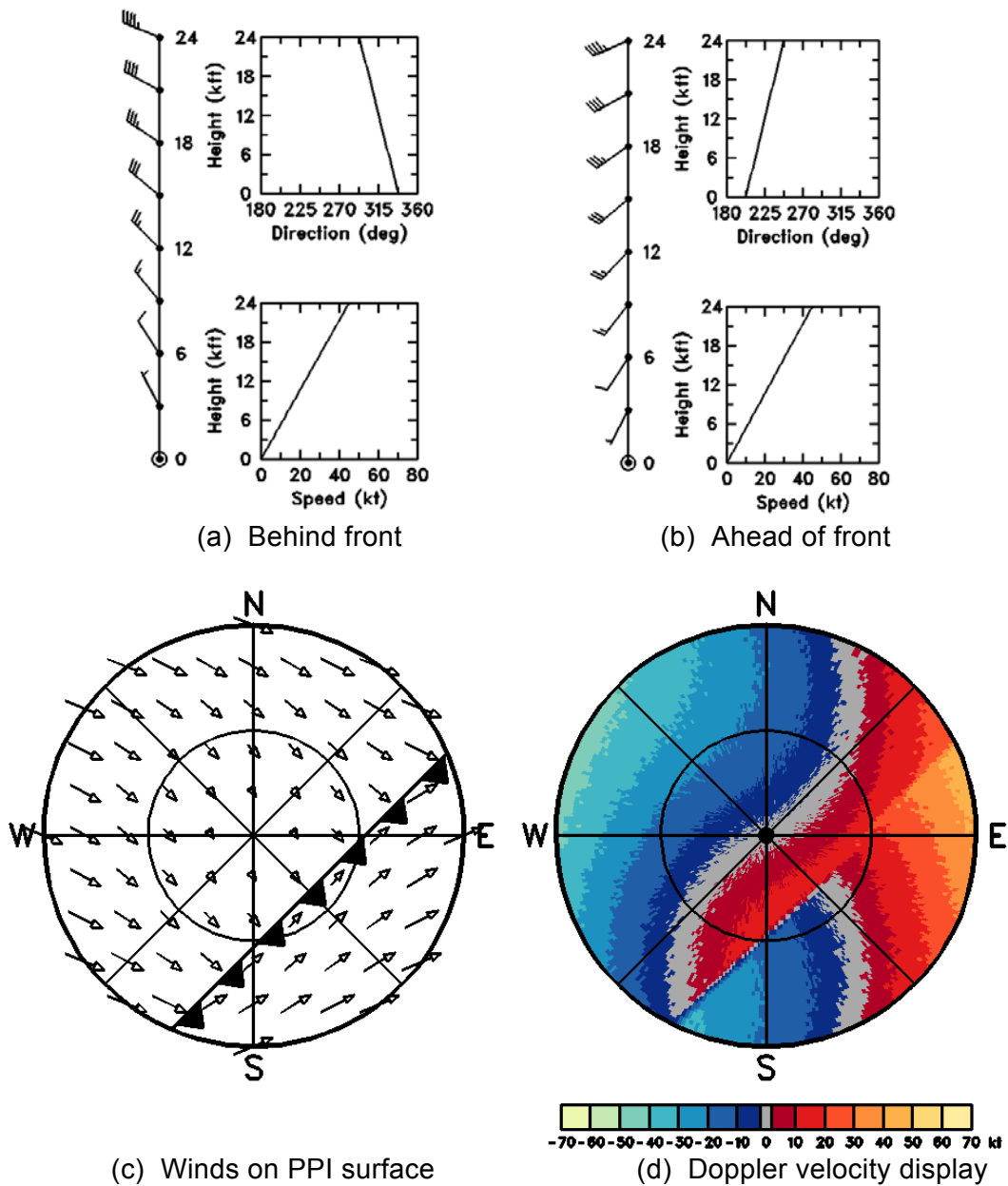
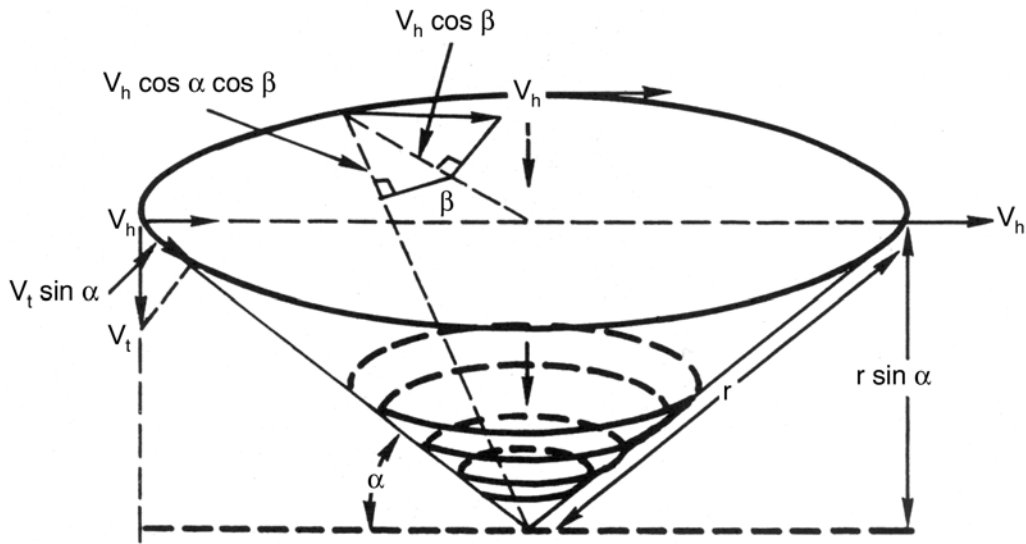
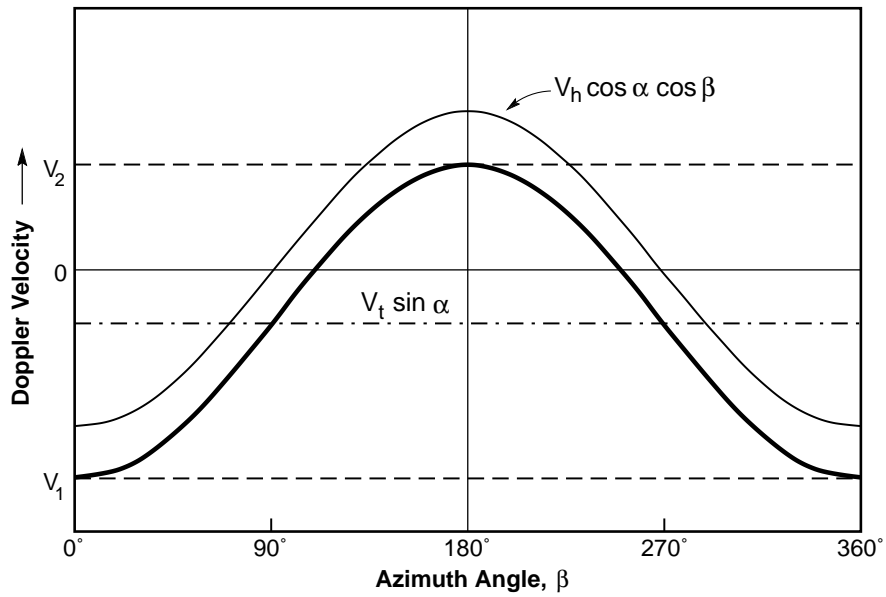


Figure 6-3
Frontal Discontinuity

Vertical profiles of (a) backing winds that increase speed with height behind front and (b) veering winds that increase speed with height ahead of front. Doppler velocity values on PPI display in (d) correspond to Doppler components of wind vectors (length proportional to speed) in (c). Positive Doppler velocities (red, orange) are away from the radar (at center of display) and negative velocities (blue) are toward the radar.



(a) Geometry of VAD scan



(b) Velocity Azimuth Display

Figure 6-4
Wind Measurements Using the VAD Technique

The thicker sinusoidal curve in (b) represents Doppler velocity values as a function of azimuth, β , measured in (a) at slant range, r , and elevation angle, α . The thicker curve is the sum of the Doppler component of the uniform environmental wind ($V_h \cos \alpha \cos \beta$, thin sinusoidal curve) and the Doppler component of the precipitation terminal fall velocity ($V_t \sin \alpha$, dash-dot line). After Atlas (1964).

If the horizontal wind and terminal fall velocity are constant around the scanning circle, Doppler velocity will vary sinusoidally as the radar antenna rotates through 360°. The plot of Doppler velocity as a function of azimuth in Figure 6-4b is called a velocity azimuth display (VAD). The sinusoidal curve will be off centered by an amount $v_t \sin \alpha$ due to the contribution of the terminal velocity of the precipitation particles. When the antenna points upwind ($\beta = 0$), the Doppler velocity value is:

$$v_1 = (v_t \sin \alpha - v_h \cos \alpha) < 0 .$$

and when the antenna points downwind ($\beta = 180^\circ$), the value is:

$$v_2 = (v_t \sin \alpha + v_h \cos \alpha) > v_1 .$$

Combining these equations, velocity at height h is:

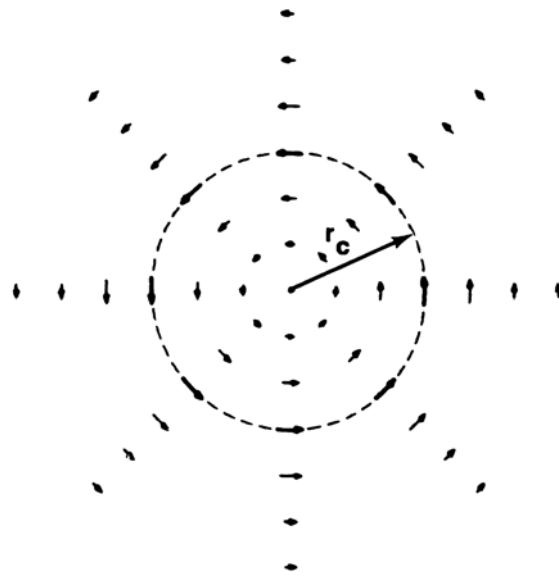
$$\hat{v}_h = \frac{v_2 - v_1}{2 \cos \alpha}$$

By making similar computations at a number of heights along the radar beam, a vertical profile of environmental winds is produced.

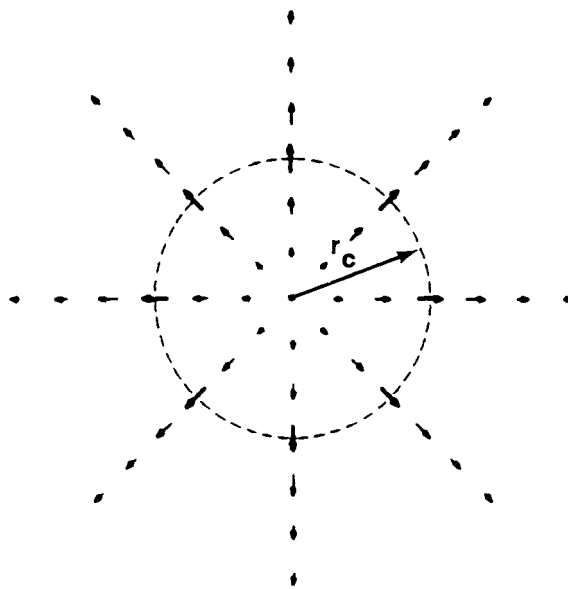
One finds that the variation of Doppler velocity with azimuth at a constant height is not exactly sinusoidal. If the terminal velocity of the scatterer is assumed to be uniform around the scanning circle (as in the case of clear air or stratiform precipitation), divergence also can be computed across the circle (Browning and Wexler 1968). This quantity is included in the VAD algorithm discussed in Part C, Chapter 3, of this Handbook.

6.4 Patterns Associated with Convective Storms. Doppler radar data collected in convective storms can be displayed in windows covering a limited area of interest. Here we display horizontal flow fields and corresponding Doppler velocity patterns within a 27 x 27 nm (50 x 50 km) window located 65 nm (120 km) due north of the radar (Figure 6-5). Except as noted, the simulated flow fields represent basic features without the addition of environmental winds and storm motion.

Horizontal variations of the wind within convective storms produce single Doppler velocity patterns that reveal important storm characteristics. Two important storm features are those of axisymmetric rotation and axisymmetric divergence as shown in Figure 6-5. In both cases, the flow is zero at the center, increases linearly to a maximum value at core radius, r_c , and then decreases beyond r_c , with the change being inversely proportional to distance from the center as indicated by the Rankine combined velocity profile in Figure 6-6.



(a) Axisymmetric rotation



(b) Axisymmetric divergence

Figure 6-5
Horizontal Axisymmetric Flow Fields

Bold arrows represent maximum wind velocities at core radius, r_c , of axisymmetric (a) rotation and (b) divergence fields having Rankine combined velocity profiles (see Figure 6-6). Vector length is proportional to speed.

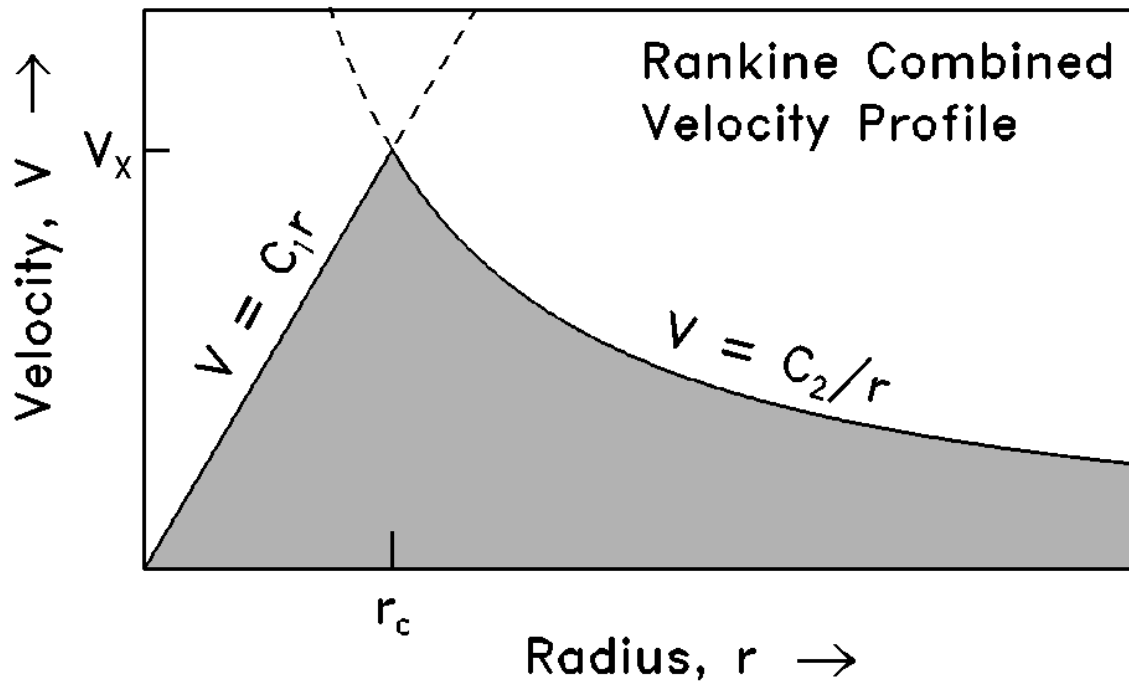


Figure 6-6
Combined Rankine Velocity Profile

Maximum velocity, V_x , occurs at core radius, r_c . Constant C_1 equals V_x/r_c and constant C_2 equals $V_x r_c$.

The rotation field in Figure 6-5a is a good approximation for the mesocyclone that is a prominent feature of the supercell stage of severe thunderstorms. When a distant Doppler radar scans through a mesocyclone to the north of the radar, patterns similar to those in Figure 6-7 are produced. Since a Doppler radar senses only the component of flow in the radar viewing direction, the gray area in Figure 6-7a represents zero Doppler velocity because flow there is perpendicular to the viewing direction. To the right of the mesocyclone center, flow is away from the radar (red, orange). To the left of the center, flow is toward the radar (blue). Whereas a Doppler radar senses none of the flow when viewing a vortex through the circulation center, it senses the complete flow on both sides of the center where flow is directly toward or away from the radar.

Therefore, the single Doppler velocity signature of a mesocyclone (or any vortex) has a pattern that is symmetrical about the radar viewing direction through the vortex center and has peak values of opposite sign at the core radius, r_c , either side of the center. When the vortex is embedded in a uniform motion field (representing some combination of environmental wind and mesocyclone movement), the circulation is no longer circular but the basic *vortex signature pattern* remains unchanged (Figure 6-7b); the only difference is that the colors have changed and the center of the signature no longer has a Doppler velocity value of zero. Note that the apparent rotation center in the combined flow field (left side of Figure 6-7b) is displaced to the left of the center of the vortex signature pattern (black dot). Algorithms that are used for detecting mesocyclones include the legacy Mesocyclone Algorithm and the more recent Mesocyclone Detection Algorithm is discussed in Part C of this Handbook.

The axisymmetric divergence field in Figure 6-5b also is a good approximation for divergence in the upper region of thunderstorm updrafts and within downdrafts near the ground. This field is reproduced in Figure 6-8a, along with the corresponding single Doppler velocity pattern. Note that the divergence signature is similar to a mesocyclone signature that has been rotated counterclockwise by 90° . Here the zero region is aligned perpendicular to the radar viewing direction because the radar does not sense motion toward the left or right of the divergence center. Maximum flows toward and away from the radar are measured along the viewing direction that passes through the divergence center; these peak velocities occur at the core radius. When the divergence field is embedded in a uniform motion field (representing some combination of environmental wind and motion of the divergence pattern), the flow field changes and the Doppler velocity values change but the basic Doppler velocity *pattern* remains unchanged.

For the mesocyclone and divergence Doppler velocity patterns discussed thus far, the radar was located 65 nm (120 km) south of the center of the flow features. When the features are much closer to the radar, the patterns become more distorted. We now investigate convergence patterns that are like divergence patterns, except that the positive and negative Doppler velocities are reversed. In Figure 6-9a, the radar is only 10 nm (19 km) south of the center of the mesocyclone (left) and the convergence region (right). The weaker Doppler velocities associated with the mesocyclone signature extend southward and converge at the radar position. The boundaries between colors in the core region are along imaginary lines radiating out from the radar location.

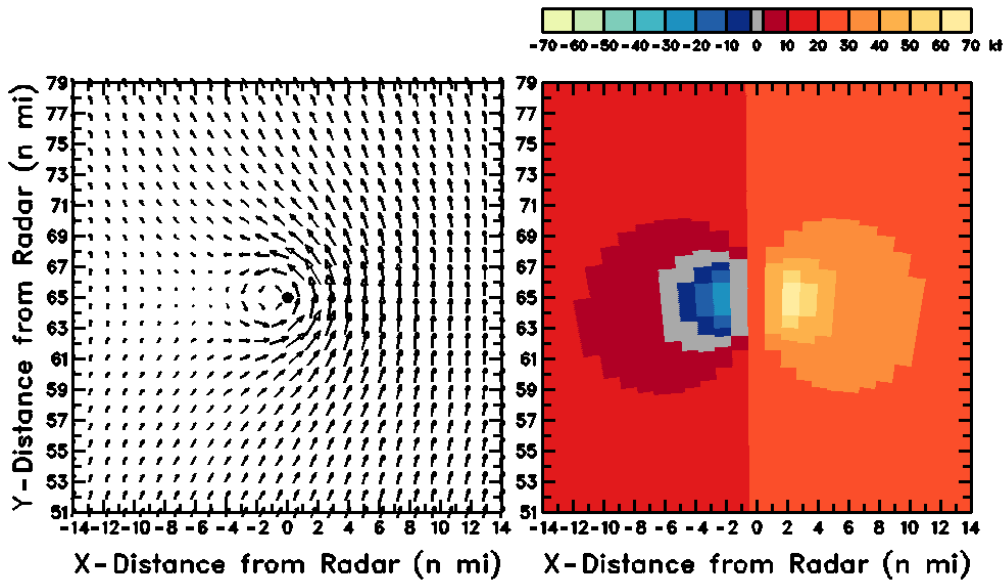
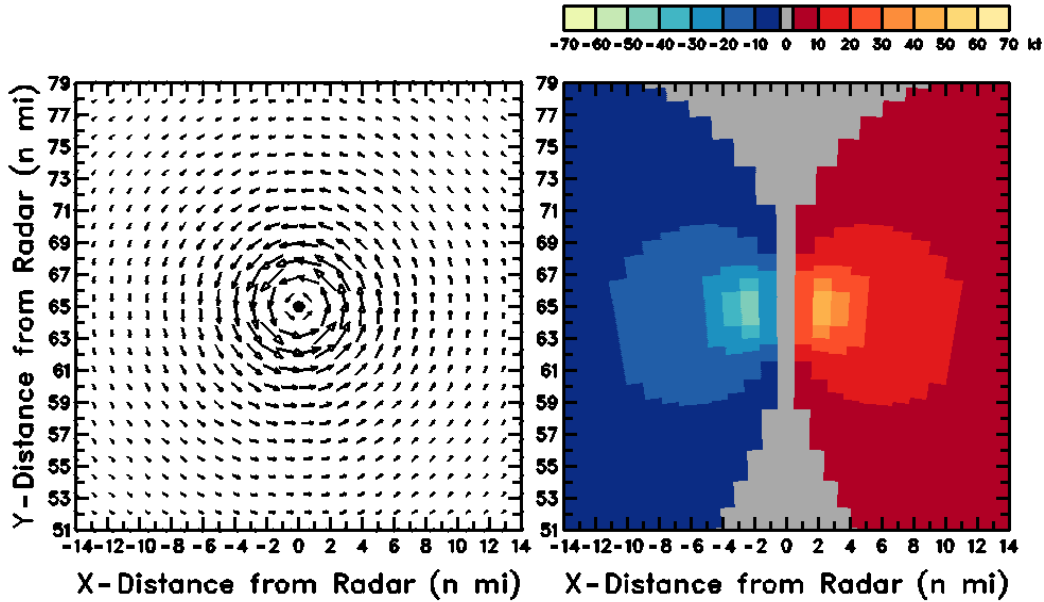
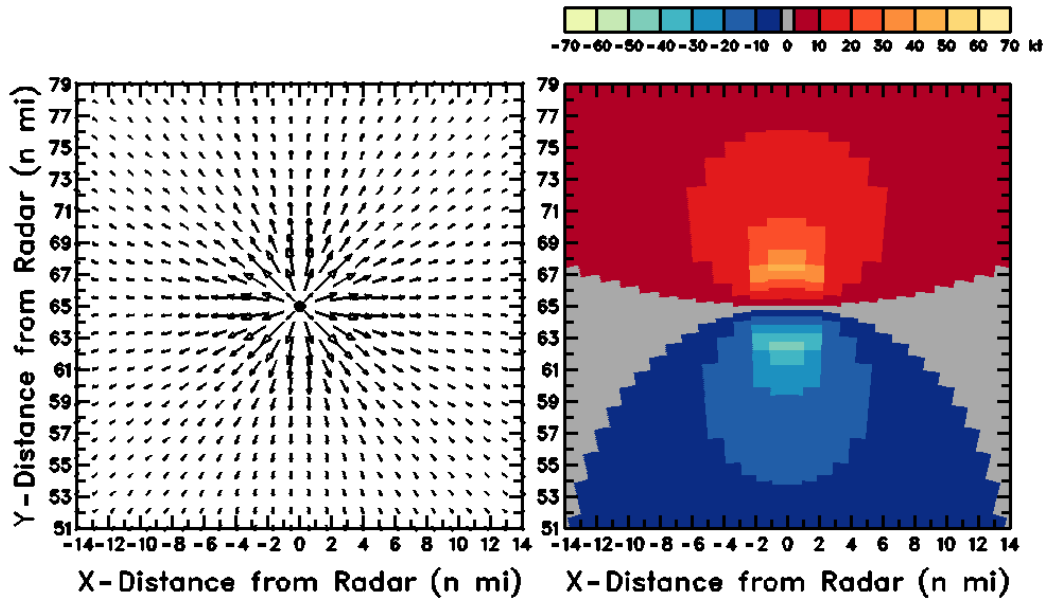
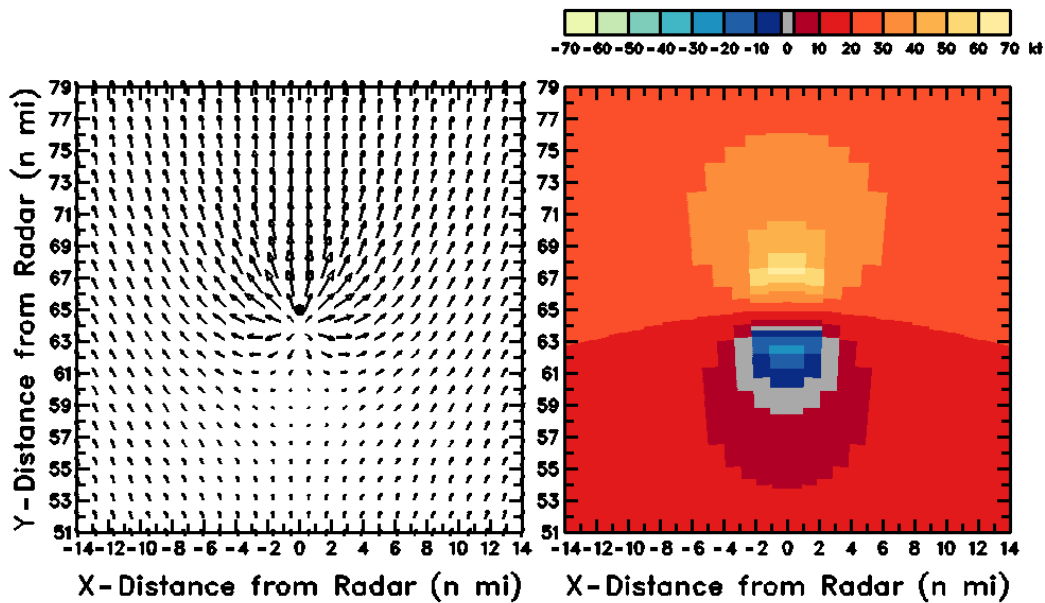


Figure 6-7
Axisymmetric Mesocyclone Signature

(a) Doppler velocity pattern for a stationary mesocyclone (right) corresponding to an axisymmetric horizontal flow field (left, dot at center) where the peak rotational velocity of 45 kts (23 ms^{-1}) is at a core radius of 2.5 nm (4.6 km). Center of panel is 65 nm (120 km) north of radar. (b) Same as (a) except for addition of a uniform motion field from the south at 20 kts (10 ms^{-1}). Vector length is proportional to speed.



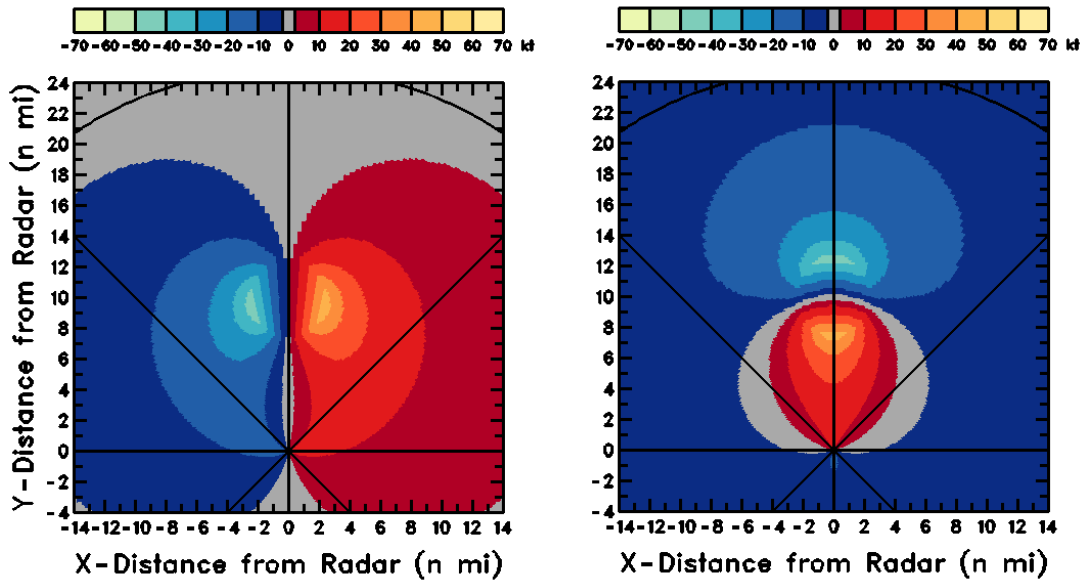
(a) Axisymmetric divergence
(b)



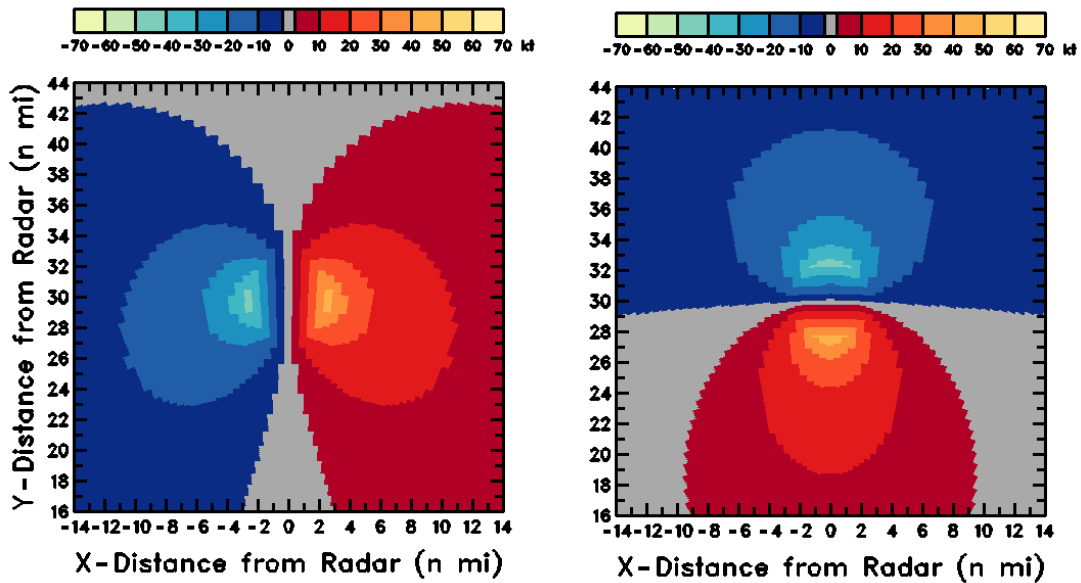
(b) Axisymmetric divergence with superimposed motion field

Figure 6-8
Axisymmetric Divergence Signature

(a) Doppler velocity pattern for a stationary region of axisymmetric divergence (right) corresponding to an axisymmetric horizontal flow field (left) where the peak radial velocity of 45 kts (23 ms^{-1}) is at a core radius of 2.5 nm (4.6 km). (b) Same as (a) except for addition of a uniform motion field from the south at 20 kts (10 ms^{-1}).



(a) Center of window 10 nm (19 km) north of radar



(b) Center of window 30 nm (56 km) north of radar

Figure 6-9
Distortion of Doppler Velocity Patterns due to Proximity of Storm to Radar

(a) Doppler velocity patterns for a mesocyclone (left) and convergence (right) when the center of the flow feature (at center of window) is 10 nm (19 km) north of the radar (located where radial lines converge). Core radii are 2.5 nm (4.6 km) and peak velocities are 45 kts (23 ms^{-1}). (b) Same as (a) except that the center of the flow feature is 30 nm (56 km) north of the radar.

The weak Doppler velocity band (gray) for convergence in the right part of Figure 6-9a has a unique shape—the center of the band (where the zero Doppler velocity contour would be located) is a circle passing through the radar and the convergence center. The chord connecting the radar and the convergence center is the diameter of the circle. From plane geometry we know that any angle inscribed in a semicircle is a right angle. Therefore, at the point along the radar viewing direction where a radial line from the radar intersects the expected circular zero Doppler velocity contour, the line is perpendicular to a convergent streamline flowing straight into the center of convergence signature.

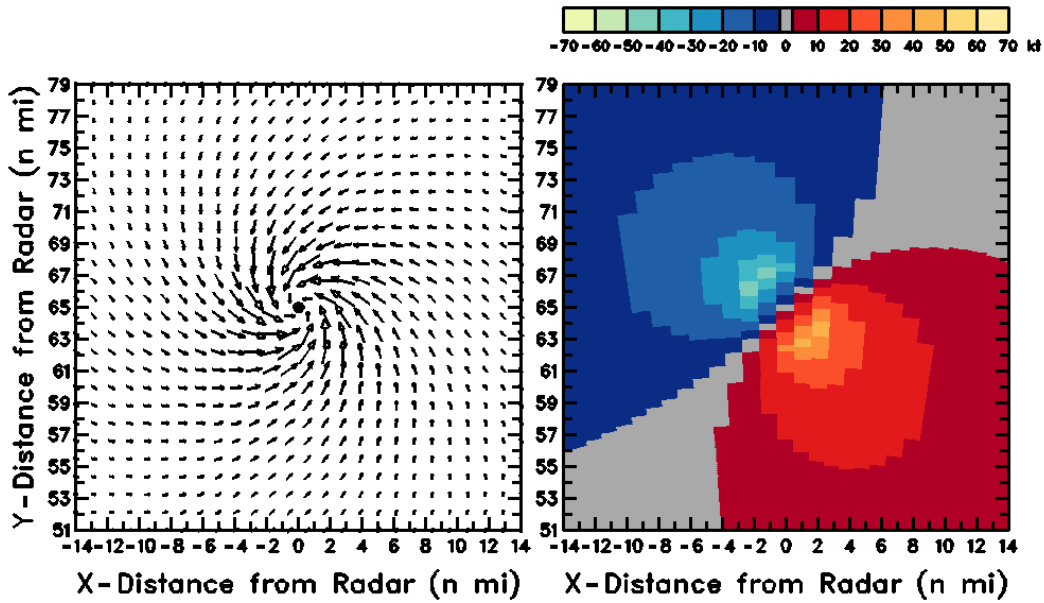
At a range of 30 nm (56 km), the mesocyclone and convergence signatures are less distorted (Figure 6-9b). The Doppler velocity areas outside the mesocyclone's core region extend southward to some extent toward the radar. For convergence, the weak Doppler velocity band is less curved since it now surrounds the circular zero Doppler velocity contour (not shown) whose diameter is 30 nm (56 km). Consequently, the positive and negative Doppler velocity regions are more nearly symmetric than those found in Figure 6-9a.

When rotation and divergence/convergence fields having the same core radius are combined, the resulting Doppler velocity pattern still resembles a Rankine velocity profile. The primary distinction is that the zero band is neither parallel to nor perpendicular to the radar viewing direction. Instead, the zero band is at an intermediate angle depending on the relative strength of the two flow field components.

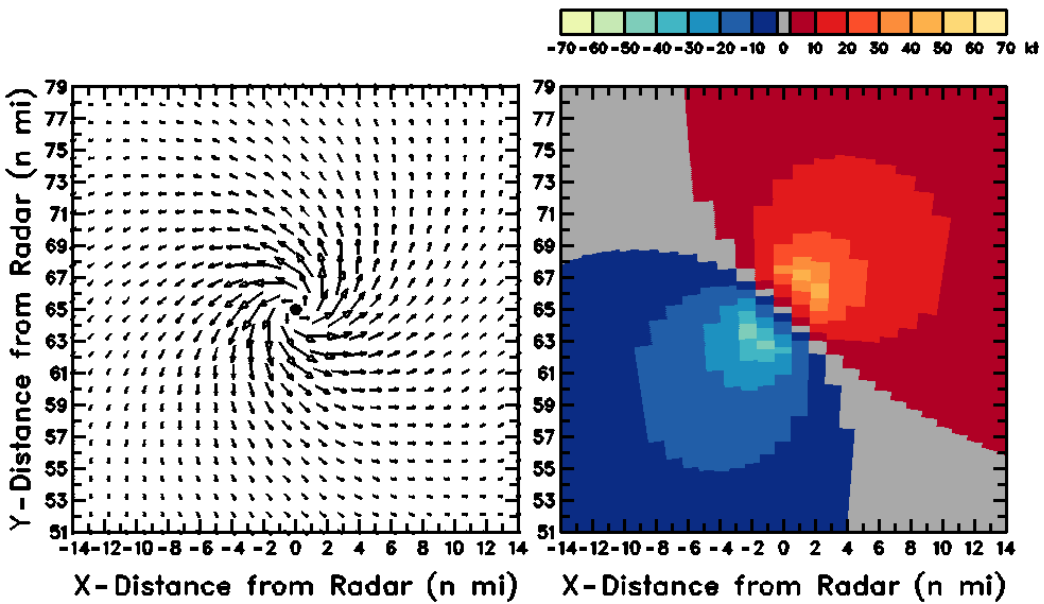
Figure 6-10a shows the combination of cyclonic rotation and convergence where the core radii are the same and the peak velocities are the same. In this case, the pattern is rotated 45°, midway between the Doppler velocity patterns for cyclonic rotation and convergence. Similarly, in Figure 6-10b the combination of cyclonic rotation and divergence is midway between the respective separate Doppler velocity patterns in Figures 6-7a and 6-8a.

The mesocyclone is the parent circulation within which significant tornadoes form. The resulting tornadoes typically are found within the mesocyclone's core region. Since all but the largest and closest tornadoes are smaller than the width of the radar beam, the tornado's rotational velocities are greatly smoothed within the beam. Doppler velocities within the resulting tornado vortex signature (TVS) do not reflect either the size or strength of the tornado but rather some indeterminable combination of the two parameters (e.g., Brown et al. 1978). The one consistent feature of the TVS is that the peak Doppler velocities toward and away from the radar are approximately one beamwidth apart.

A strong TVS is simulated at the edge of the core region of the parent mesocyclone in Figure 6-11a. Though it is small, the TVS is a prominent feature where the packing of colors represent extreme Doppler velocity values of opposite sign. The presence of a strong TVS located 0.5 nm (0.9 km) east of the parent mesocyclone, as illustrated in Figure 6-11b, also is very evident within the parent mesocyclonic circulation. Owing to the smearing effect of an ever-widening radar beam with increasing range, a tornado of a given size and strength produces a Tornado Vortex Signature (TVS) that is progressively weaker with increasing distance from the radar. Only the strongest tornadic vortex signatures are evident beyond 60–70 nm (111–130 km) from a WSR-88D.



(a) Axisymmetric cyclonic rotation and convergence

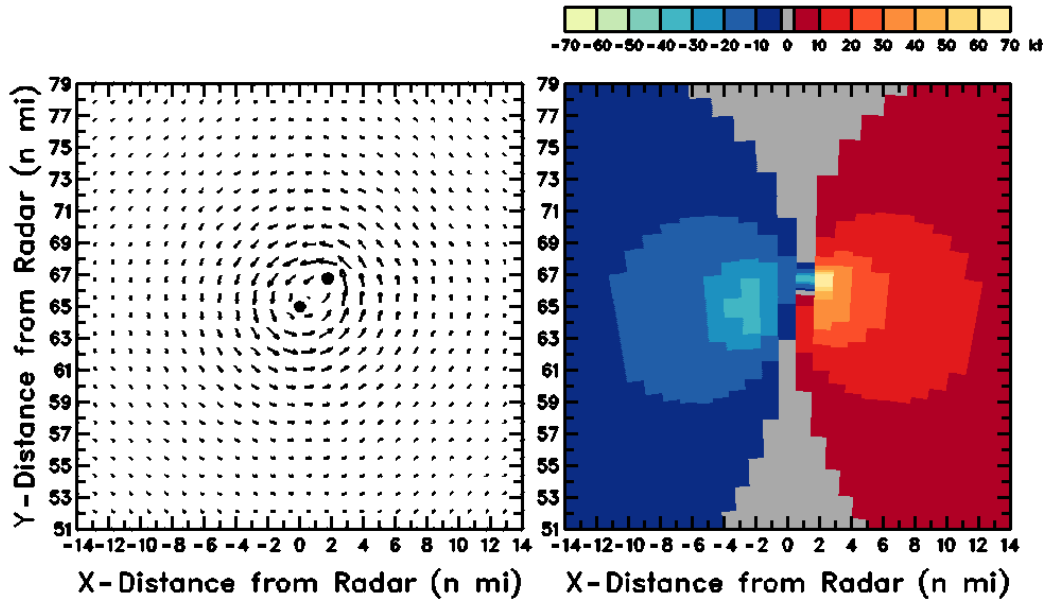


(b) Axisymmetric cyclonic rotation and divergence

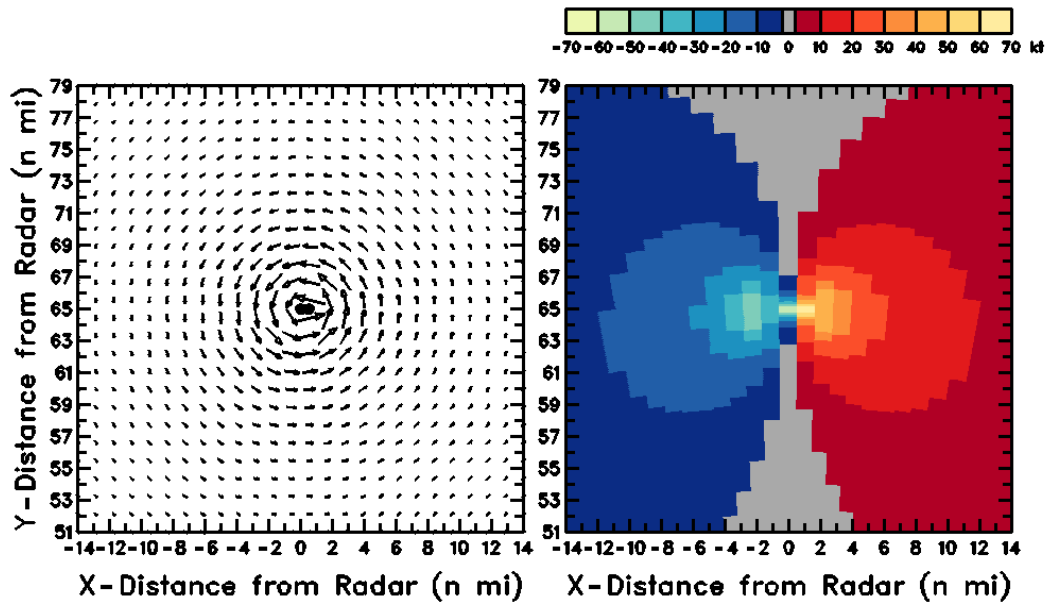
Figure 6-10

Combinations of Axisymmetric Rotation and Convergence/Divergence

(a) Doppler velocity pattern (right) corresponding to combination of convergence and cyclonic rotation fields (left) having same core radii 2.5 nm (4.6 km) with maximum inflow velocity equaling maximum rotational velocity 31.8 kts (16.4 ms^{-1}). Dot in left panel is center of combined flow. (b) Same as (a) except for combination of divergence and cyclonic rotation.



(a) TVS at edge of mesocyclone core region



(b) TVS located 0.5 nm (0.9 km) east of mesocyclone center

Figure 6-11
Tornadic Vortex Signature within Mesocyclone Signature

(a) Doppler velocity pattern (right) corresponding to a TVS (peak rotational velocity of 60 kts (31 ms^{-1}), core radius of 0.5 nm (0.9 km) located 2.5 nm (4.6 km) northeast of the mesocyclone center (peak rotational velocity of 35 kts (18 ms^{-1}), core radius of 2.5 nm (4.6 km). (b) Same as (a) except that TVS is located within core region 0.5 nm (0.9 km) east of mesocyclone center.

6.5 Concluding Remarks. The Doppler velocity patterns presented in this chapter represent some of the more straightforward patterns that will be encountered. The development of expertise in display interpretation requires detailed training and extensive experience. The basic principles that have been presented in this chapter can be used to infer the basic components of the observed flow.

REFERENCES

- Atlas, D., 1964: Advances in radar meteorology. *Adv. Geophysics*, **10**, Academic Press, 317–478.
- Battan, L. J., 1973: *Radar Observations of the Atmosphere*, University of Chicago Press, 323 pp.
- Brown, R. A., and V. T. Wood, 1991: On the interpretation of single-Doppler velocity patterns within severe thunderstorms. *Wea. Forecasting*, **6**, 32–48.
- Brown, R. A., L. R. Lemon, and D. W. Burgess, 1978: Tornado detection by pulsed Doppler radar. *Mon. Wea. Rev.*, **106**, 29–38.
- Browning, K. A., and R. Wexler, 1968: The Determination of kinematic properties of a wind field using Doppler radar. *J. Appl. Meteor.*, **7**, 105–113.
- Donaldson, R. J., Jr., 1970: Vortex signature recognition by a Doppler radar. *J. Appl. Meteor.*, **9**, 661–670.
- Doviak, R. J., and D. S. Zrnić, 1993: *Doppler Radar and Weather Observations*, 2nd ed., Academic Press, 562 pp.
- Wood, V. T., and R. A. Brown, 1986: Single Doppler velocity signature interpretation of nondivergent environmental winds. *J. Atmos. Oceanic Technol.*, **3**, 114–128.